Available online at www.elixirpublishers.com (Elixir International Journal)

Mechanical Engineering

Elixir Mech. Engg. 65 (2013) 19864-19872

ISSN: 2229-712X

FSW of Aluminium alloys – Energy model for taper tool geometry

D.Muruganandam[1,*], D.Raguraman[1], B.Senthilkumar[1] and Susil Lal Das[2]

[1]Sri Sai Ram Engineering College, Chennai – 600044.

[2]Jeppiaar Engineering College, Chennai – 600119.

$$Min \sum_{i=1}^{n} w_i . x_i$$

$$A_{(n+w)\times n} X_{n\times 1} \geq b_{(n+w)\times 1}$$

$$Min \sum_{i=1}^{n} w_i . x_i$$

$$s.t \quad y = A_{n\times n} X_{n\times 1} \geq b_{n\times 1}$$

ARTICLE INFO

Article history:
Received: 4 December 2013;
Received in revised form:
6 December 2013;
Accepted: 9 December 2013;

Keywords
Friction-stir welding,
Energy,
Aluminum Alloys.

ABSTRACT

Friction-stir welding has received a huge interest in the last few years. The many advantages of this promising process have led researchers to present different theoretical and experimental explanation of the process. The way to quantitatively and qualitatively control the different parameters of the friction-stir welding process has not been paved. In this study, a refined energy based model that estimates the energy generated due to friction and plastic deformation is presented. The effect of the plastic deformation at low energy levels is significant and hence a scale factor is introduced to control its effect. The predicted heat energy and the obtained maximum temperature using the present model are compared to the theoretical and experimental results available in the literature and a good agreement is obtained.

Introduction

The energy required to bond two components by welding is usually provided by direct heat. The two common sources of direct heat are those derived from either a chemical reaction or electrical energy. The exception includes explosive bonding, which uses the kinetic energy released from the impact of a moving object with a stationary target and friction-stir welding, which combines frictional heating at the interface with the localized plastic deformation within the material. Friction-stir welding (FSW) is a solid-state joining process that enables welding hard-to-wild metals such as high-strength aluminum alloys. Friction-stir welding was developed and patented by The Welding Institute (TWI) in 1991 [1]. Since then the research efforts to understand the micro and macro mechanics of the process are continuous. During FSW, no melting point occurs, and as a result the process is performed at much lower temperatures than conventional welding processes. This has a direct impact on the safe application of the FSW to the environment. Among the advantages of the FSW are [2]

• Low distortion, even in long welds
• Excellent mechanical properties as proven by fatigue, tensile and bend tests
• No arc
• No fume
• No porosity
• No spatter
• Low shrinkage
• Energy efficient
• Non-consumable tool; one tool can typically be used for up to 1000m of weld length in 6000 series aluminum alloys
• No filler wire
• No gas shielding for welding aluminum
• No grinding, brushing or pickling required in mass production
• Can weld aluminum and copper of more than 50mm thickness in one pass.

However, as of the present time, there are some limitations, which include

• Work pieces must be rigidly clamped
• Backing bar required, when self-reacting tool or directly opposed tools are not available.

Tele:
E-mail addresses: murudurai@gmail.com

• Keyhole at the end of each weld.

• Cannot make joints which require metal deposition (e.g. fillet welds)

Friction-stir welding is carried out using a rotating tool that is attached to a shoulder piece and the whole unit is translating over the line of welding. The rotation and translation of the pin within and on top of the line of welding generates heat, which is used to weld the workpieces. Heat is generated due to plastic deformation of the workpiece and the effect of the friction between the surfaces of the tool and the workpiece [3,4]. Figure 1 is a schematic of the friction stir welding process. According to most of the literature, the weld zone around the tool is divided into four regions: unaffected or parent metal, heat affected zone (HAZ), thermo-mechanically affected zone (TMAZ), and weld nugget. The unaffected material is remote from the weld, which has not experienced deformation or it may have healed after being experienced a thermal cycle. The heat affected zone (HAZ), which was previously referred to as thermally affected zone, is in the neighborhood of the weld center and its microstructure and mechanical properties have been modifies as a result of experiencing a thermal cycle. This zone does not associate a plastic deformation. Thermo-mechanically affected zone (TMAZ) is plastically deformed due to the friction-stir welding tool and its microstructure is modified due to the generated heat. Finally, the weld-nugget zone is the recrystallized area in the TMAZ.

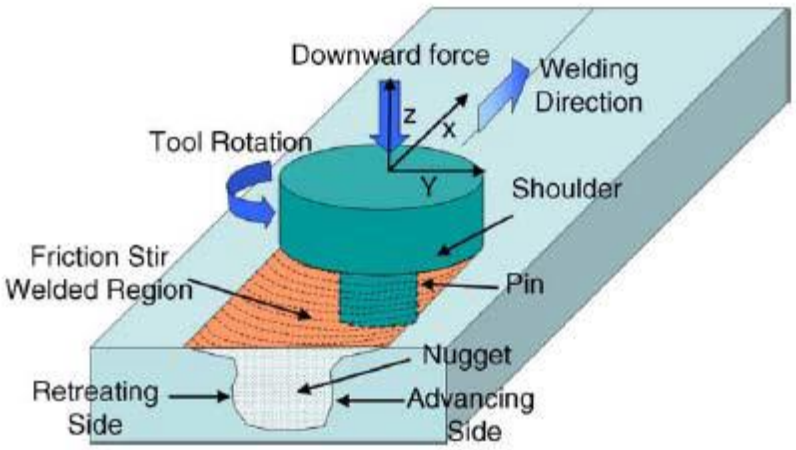

Fig. 1 A schematic of friction-stir welding process

Modeling of FSW was presented by many authors. Bendzsak [5] used the finite volume method to compute the flow of the workpiece around the tool. Askari et al. [6] used an elasto-visco plastic model to estimate the material flow around the tool. A thermo-mechanical model was presented by Heurtier et al. [7] who analytically determined the flow pattern around the tool in order to calculate the effective strain in the deformed plastic zone. To achieve the same purpose, the finite element method [8-10] and the finite difference method [11] were used. Muruganandam et al. used Tauguchi technique for the identification of rotational speed for higher strength using cylindrical and taper model[12]. In the present work, a simple energy-based model for the friction stir weld is proposed for taper pin. The model aims at estimating the heat generated due to plastic deformation within the work pieces and friction between the tool surfaces and the work pieces. This generated energy and the associated maximum temperature are compared to the results available in the literature to verify the proposed model.

The proposed energy model

Previous studies [3] assume that heat generated due to friction of the pin shoulder on the work piece surface is dominant and the heat generated due to the plastic deformation within the work piece and the friction of the pin of the material is negligible. However, other authors e.g. Heurtier et al. [3] and Hamilton et al. [13] consider the heat generated from both the friction of the pin shoulder and plastic flow. In fact, the energy due to plastic deformation and friction of the shoulder with the surface of the work piece are related and competing each other. As the heat generated by the shoulder is low, the flow stress is higher and hence the resulting plastic deformation energy increases. On the other hand, as the heat generated by the shoulder is high, the flow stress reduces and as a result

the plastic strain contribution decreases. In this work, heat is modeled to be generated by the friction of the shoulder and plastic deformation. Figure 2 presents a schematic of the friction-stir welding tool. It is assumed that the tool rotates with an angular speed of ω and transversely translates along the line of welding with a speed of v_o . The tool is acted upon by a compressive force F, as shown in the figure.

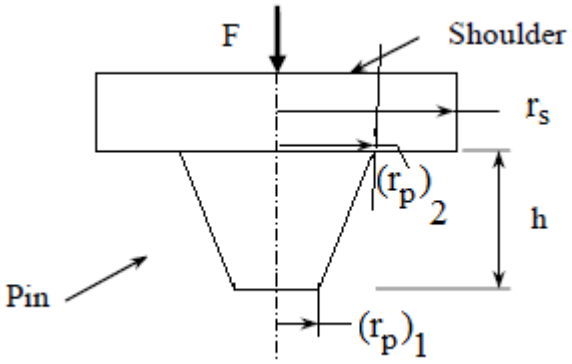

Fig 2. Geometry of the FSW tool

Following, Hamilton et al. [12], the energy generated per unit length of the weld E is given by

$$E_f = P_f / vo \tag{1}$$

Where P is the total power generated by friction. Assuming that the total torque due to friction of the pin, shoulder, and pin circumference with the work piece surfaces is T_f , the frictional power is then given by

$$P_f = T_f \omega \tag{2}$$

Where ω is the pin angular speed. To find an expression for the total frictional torque T_f , we let

$$T_f = T_s + T_p \tag{3}$$

Where T_s is the torque generated by the shoulder and T_p is torque generated by the pin. Assuming that a uniform shear stress τ occurs during welding, we obtain

$$\int_{(r_p)_2}^{r_s} \tau(2\pi r) r\,dr + \int_{0}^{(r_p)_1} \tau(2\pi r) r\,dr + \tau\left(\frac{2}{3}\pi\left[\left([r_p]_1 + \left([r_p]_2\right]h\right)([r_p]_2 \tag{4}$$

Where r_s is the radius of the shoulder, $([r_p]_1 \; and \; ([r_p]_2$ is the radius of the pin, and h is the height of the pin, as shown in Fig. 2. Equation 3 reduces to

$$T_f = \frac{2}{3}\pi\tau\,([r_p]_2{}^2\left[\frac{(r_s)^3}{([r_p]_2{}^2} - (r_p)_2 + \frac{\left((r_p)_1\right)^3}{([r_p]_2{}^2} + \frac{(r_p)_1 + (r_p)_2}{(r_p)_2}\,h\right] \tag{5}$$

Assuming a coefficient of friction is μ , the total friction force F_f due to the compressive force F is given by

$$F_f = \mu F \tag{6}$$

Noting that $\pi([r_p]_2{}^2\tau$ is the total friction force, Eq. 3 yields

$$T_f = \frac{2}{3}\mu F\left[\frac{(r_s)^3}{([r_p]_2{}^2} - (r_p)_2 + \frac{\left((r_p)_1\right)^3}{([r_p]_2{}^2} + \frac{(r_p)_1 + (r_p)_2}{(r_p)_2}\,h\right] \tag{7}$$

Substituting Eq. 5 into Eqs. 1 and 2, we obtain

$$E_f = \frac{2}{3}\mu F \left[\frac{(r_s)^3}{\left([r_p]_2\right)^2} - (r_p)_2 + \frac{\left((r_p)_1\right)^3}{\left([r_p]_2\right)^2} + \frac{(r_p)_1 + (r_p)_2}{(r_p)_2}\, h \right] \frac{\omega}{v_o} \tag{8}$$

Equation 8 defines the energy per unit length of the weld due to friction between the tool and the work piece. For a given tool geometry, tool speed, and work piece material, this energy can be easily identified. As can be noted from Eq. (1), the power generated due to friction is given by

$$P_f = \frac{2}{3}\mu F \left[\frac{(r_s)^3}{\left([r_p]_2\right)^2} - (r_p)_2 + \frac{\left((r_p)_1\right)^3}{\left([r_p]_2\right)^2} + \frac{(r_p)_1 + (r_p)_2}{(r_p)_2}\, h \right] \omega \tag{9}$$

Frigaard [14] reported that the coefficient of friction between aluminum and mild steel should be set as the average value between 0.5 for sticky friction and 0.25 for dry sliding. Hamilton [13] used 0.5 as an initial value for the coefficient of friction, and then reduces it as the energy level increases. For instance, they reduced the coefficient of friction to 0.45 when the energy level exceeds 2000 J/mm and 0.4 for an energy level exceeding 3000 J/mm. In this study, a coefficient of friction of 0.5 is used.

The other source of heat is due to the plastic deformation within the work piece. Provided that the plastic deformation within the work piece is totally transformed into heat, the heat generated due to plastic deformation per unit weld length can be expressed as follows:

$$E_p = \sigma\varepsilon\, V \tag{10}$$

where σ and ε are the stress and strain, respectively, V = is the volume per unit length of the base material.

The stress σ is given by

$$\sigma = K\varepsilon^n \exp\left(\frac{mQ}{R_G T}\right) \tag{11}$$

where *K* is the strength coefficient, *n* is the strain hardening exponent, *m* is the strain rate sensitivity, *Q* is the apparent activation energy, R_G is a constant equals 8.32 J mol-1K−1, and *T* is the absolute temperature. As a result, the energy generated due to plastic deformation per unit length of the weld is expressed as follows:

$$E = K\,\varepsilon^{n+1}\; bl\mathbf{h} \exp\left(\frac{mQ}{R_G T}\right) \tag{12}$$

The stress-strain relationship in the room temperature for AA2024, AA7075 and AA 6061 are shown in this figure 3.

Because the temperature is already unknown, the accurate calculation of the plastic strain energy needs an iterative process. Since the effect of the energy due to plastic deformation is much smaller than that due to friction, a simple model was proposed as follows:

$$E_p = \sigma_e \varepsilon_e\, bl\mathbf{h} \tag{13}$$

where σ_e is the equivalent (effective) stress and ε_e is the effective strain. Using the finite element method, Heurtier et al. [3] found that the effective strain is around six. In this case, the effective stress is assumed to be constant, and hence the area under the curve becomes a rectangle. The power generated due to the plastic deformation is given by

$$P_p = \sigma_e \varepsilon_e bl\mathbf{h}\; v_o \tag{14}$$

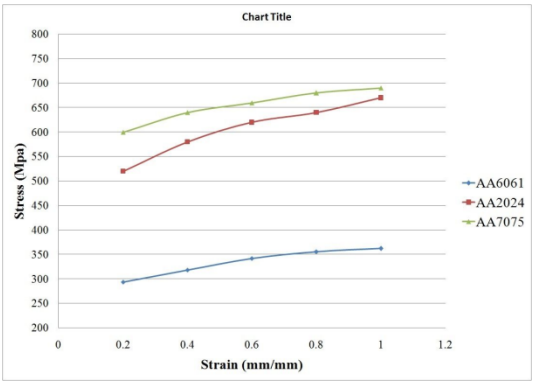

Fig 3. True-stress true-strain curve for AA 2024,AA7075 and AA6061.

The total energy generated per unit length of the wild is the sum of the energy generated due to friction between the tool and the workpiece surface and the plastic deformation within the workpiece.A scaling factor is introduced in order to control the effect of the energy due to plastic deformation. At low levels of heat generation, the plastic deformation plays a significant role. As the frictional heat becomes larger, the effect of the plastic deformation diminishes. Hamilton et al. [13] reported three regions based on the experimental results available in the literature. For energy levels below 800 J/mm, heat generation due to plastic deformation dominates heat generation due to friction. For energy levels greater than 2000 J/mm, frictional slip occurs due to the material softening. In the region in between, both sources of heat are considerable. Based on that, the scale factor, as presented in Fig. 4, is proposed in this study.

As a result, the total energy generated can be expressed as follows:

$$E = E_f + s\,E_p = \frac{2}{3}\mu F\left[\frac{(r_s)^3}{([r_p])_2^2} - (r_p)_2 + \frac{(r_p)^3}{([r_p])_2^2} + \frac{(r_p)_1 + (r_p)_2}{(r_p)_2}\,h\right]\frac{\omega}{v_o} + s\,\sigma_e\varepsilon_e\; blh \qquad (15)$$

where the scale factor *s* is shown in Fig. 4. The total power generated is given by

$$P = E\,V_o = \frac{2}{3}\mu F\left[\frac{(r_s)^3}{([r_p])_2^2} - (r_p)_2 + \frac{(r_p)^3}{([r_p])_2^2} + \frac{(r_p)_1 + (r_p)_2}{(r_p)_2}\,h\right]\omega + s\,\sigma_e\varepsilon_e\,(blh)\;v_o \qquad (16)$$

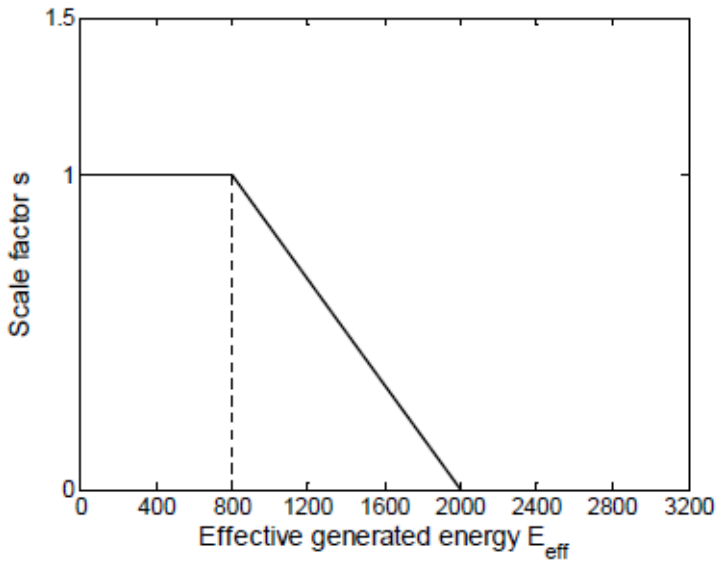

Fig 4. The proposed scale factor to control the heat due to plastic deformation

The term effective energy is introduced to take into account the case where the height of the FSW tool pin *h* is different from the thickness of the workpiece *t*. The effective energy is defined as follows:

$$E_{eff} = \frac{h}{t}E = \beta E \quad (17)$$

where β is the coefficient of transfer efficiency.

Results and discussion

The energy model proposed in the previous section accounts for both the frictional heating and the heating results from the plastic deformation. In order to validate the model, the total energy presented in taper model is adopted into the empirical formula developed by Hamilton et al. The formula is obtained from the experimental results available in the literature. The empirical formula is given by

$$\frac{T_{max}}{T_s} = 1.56\ X\ 10^{-4}\ E_{eff+0.54} \quad (18)$$

where T_{max} is the maximum temperature generated within the weld, *T*s is the solidus temperature in Kelvin, E_{eff} is the effective energy generated per unit length of weld in J/mm as given in Eq. (18). The non dimensionlized maximum temperature is obtained so that the deduced formula can serve for the AA6000 and AA7000 series considered in the study.A good agreement is obtained except in the low-energy level region. The reason is that Hamilton et al. neglected the energy generated by the plastic deformation, which is significant when the frictional heating is low. In the present taper model, the heating due to plastic deformation has been taken into consideration through the scaling factor as given by Eq. (15). To validate this taper model, we find the total energy generated for given welding parameters and solved for the maximum temperature. The obtained maximum temperature is then compared to both the cylindrical model and the taper model. It is found out that considering the heat due to plastic deformation enabled this model to better fits the experimental results at all energy levels. Three aluminum alloys are considered using different welding parameters such as tool geometry and welding speed. Table 1 presents the three alloys with the material characteristics and tool geometry used for each case.

Table I. Material characteristics and tool geometry of the aluminum Alloys used

Aluminium alloy		**6061 - T6**	**2024 - T6**	**7075 - T6**
Ref.		L1	L2	L3
t (mm)		6	6	6
ρ (kg/m^3)		2700	2780	2810
C_p (J/Kg K)		896	875	960
K (W/m K)		167	177	130
α (x 10^{-6} cm/cm/C)		23.4	22.8	23.2
T_s (K)		855	910	748
Tool geometry	r_i (mm)	12.0	12.0	12.0
	r_o(mm)	9.5	9.5	9.5
	h (mm)	6.0	6.0	6.0

Welding parameters including the tool rotational speed, tool translational speed, and the acting normal force are given in Table 2.A comparison between the heat energy obtained by cylindrical model and the heat energy obtained using the proposed taper model in this study is given in Table 3. Investigating these results, one notes that at low-energy levels, , the model of plastic deformation estimates the generated energy. This is expected since the plastic deformation is significant in this region, which is ignored in the model at higher energy level due to scaling factor close to zero. On the other hand, the energy predicted using present taper model seems much greater than the cylindrical model, which reflects the enhancement of the model by including the plastic deformation. Moreover, in the high energy level, up to 2000 J/mm, the results are very close. The graphs (Fig.5 and fig.6) are plotted between the rotational speed and effective energy for both the cylindrical and taper model. By data interpretation it is clear that the change in tool geometry from cylindrical shape to taper shape increases the effective energy. However, the model is mainly based on geometry so the change in material is not much effected the effective energy.

Table II: Welding Rotational And Translational Speeds And The Applied Normal Force

Alloy	Case	R.P.M.	v_o (mm/s)	F (KN)
AA 6061 – T6	1	200	1.5	10
	2	400	1.5	10
	3	600	1.5	10
	4	800	1.5	10
	5	1000	1.5	10
	6	1200	1.5	10
AA 2024 – T6	7	200	1.5	10
	8	400	1.5	10
	9	600	1.5	10
	10	800	1.5	10
	11	1000	1.5	10
	12	1200	1.5	10
AA 7075 – T6	13	200	1.5	10
	14	400	1.5	10
	15	600	1.5	10
	16	800	1.5	10
	17	1000	1.5	10
	18	1200	1.5	10

Table III: Energy And Maximum Temperature Obtained Using Taper Model And Cylindrical Model.

Case #	E (J/mm) – cylindrical model	E (J/mm) – Taper model	T_{max} – cylindrical model	T_{max} – Taper model
1	975	1574	114	129
2	1881	2467	137	150
3	2824	3703	160	181
4	3760	4932	183	211
5	4702	6168	207	241
6	5643	7401	230	271
7	988	1587	121	137
8	1883	2469	145	159
9	2826	3705	170	191
10	3772	4944	195	223
11	4716	6181	220	255
12	5659	7418	244	287
13	1019	1618	90	101
14	1894	2480	107	117
15	2835	3714	125	141
16	3778	4950	143	164
17	4718	6184	161	188
18	5659	7417	179	211

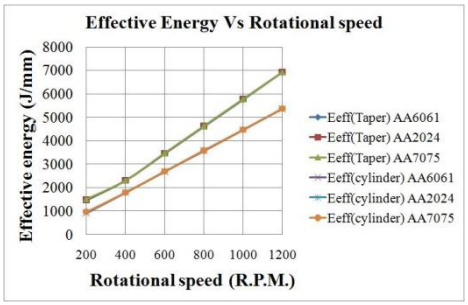

Fig 5. Variation of the effective energy with rotational speed for cylindrical and taper model

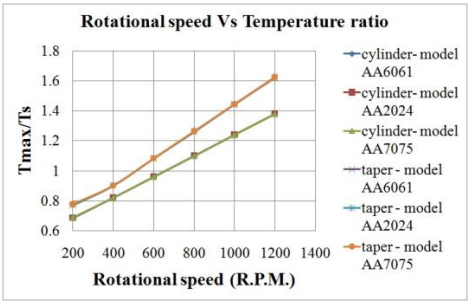

Fig 6. Variation of the temperature ratio with rotational speed for cylindrical and taper model

Conclusions

In this study, a simple model that estimates the energy generated in friction-stir welding is presented. The model accounts for the heat generated due to friction between the weld tool and the surface of the workpiece and heat generated due to plastic deformation. The later is scaled such that its effect becomes significant at low-energy levels. To account for the possible difference between the tool height and the thickness of the workpiece, a transfer efficiency coefficient is introduced in order to obtain an effective energy for the process. Based on an empirical formula that is based on experimental results, the maximum temperature in the weld and the effective energy is identified for both the cylindrical and taper model. A comparison between the heat energy and maximum temperature ratio are obtained using the proposed model. The heat due to plastic deformation is found to have a significant effect on the resulting temperature especially at low-energy levels. This model can be enhanced by considering an accurate model for the plastic deformation that will automatically predicts the heat generation due to plastic deformation at different energy levels. This will automatically eliminate the scale factor introduced in this study. Moreover, an accurate thermal model that simulates the heat transfer within and around the weld tool could be used.

References

[1] W. M Thomas, "Friction Stir Butt Welding", International Patent Application PCT/GB92, Patent Application GB125978.8, 1991.

[2] The Welding Institute Website: www.twi.co.uk

[3] P. Heurtier, M. J. Jones, C. Desrayaud, J. H. Driver, F. Fontheillet, and D. Allehaux, "Mechanical and Thermal Modeling of Friction Stir Welding", Journal of Materials Processing Technology, Vol. 171, pp. 348-357, 2006.

[4] R. S. Mishra, and Z. Y. Ma, "Friction Stir Welding and Processing", Materials Sciences and Engineering, R 50, pp. 1-78, 2005.

[5] G. J. Bendzsak, T. H. North, and C. B. Smith, "An Experimentally 3D Model for Friction Stir Welding", 2nd International Symposium 'Friction Stir Welding', TWI Ltd., Gothenburg, Sweden, 2000.

[6] Askari, S. Silling, B. London, and M. Mahoney, "Modeling and Analysis of Friction Stir Welding Processing", K. V. Jata, et al. (Eds.), Friction Stir Welding and Processing, TMS, Warrendale, PA, pp. 43-54, 2001.

[7] P. Heurtier, C. Desrayaud, and F. Montheillet, "A Thermomechanical Analysis of the Friction Stir Welding Process", Materials Science Forum, Trans. Tech. Publications, Switzerland, pp. 1537-1542, 2002.

[8] S. Xu and X. Deng, "Two and Three Dimensional Finite Element Models for the Friction Stir Welding Process", 4th Int. Symp. On Friction Stir Welding, TWI Ltd., Park City, Utah, USA, 2003.

[9] P. Dong, F. Lu, J.K. Hong, and Z. Cao, "Coupled Thermomechanical Analysis of the Friction Stir welding Process using Simplified Models", Science Technology Welding and Joining, Vol. 6, pp. 281-287, 2001.

[10] P. Ulysse, "Three-Dimensional Modeling of Friction Stir Welding Process", International Journal of Machine Tools and Manufacture, Vol. 42, pp. 1549-1557, 2002.

[11] F. Palm, U. Hennebohle, V. Erofeev, E. Earpuchin, and O. Zaitzev, "Improved Verification of FSW-Process Modeling relating to the Origin of Material Plasticity", 4th Int. Symp. On Friction Stir Welding, TWI Ltd., Metz, France, 2004.

[12] D.Muruganandam, D.Raguraman, and Sushil Lal Das, "Analysis of mechanical strength of dissimilar aluminium alloys AA7075 and AA2024 in friction stir welding using Taguchi's technique", International Journal of Research in Aeronautical and Mechanical

Engineering, Vol.1,Issue 6, pp. 13-22, 2013. [13] Hamilton, S. Dymek, and A. Sommers, "A Thermal Model of Friction Stir Welding in Aluminum Alloys", International Journal of Machine Tools and Manufacture, Vol. 48, pp. 1120-1130, 2008.

[14] O. Frigaard, O. Grong, and O. T. Milding, "Modeling of Heat Flow Phenomena in Friction Stir Welding of Aluminum Alloys", Proceedings of the 7th International Conference in Joints in Aluminum, Vol. S16, 1998.

[15] P. A. Colgrove, and H. R. Shercliff, “Experimental and Numerical Analysis of Aluminum Alloy 7075-T7351 Friction Stir Welds”, Science and Technology of Welding and Joining, Vol. 8, pp. 360-368, 2003.

[16] M. Z. Khandkar, J. A. Khan, and A. P. Reynolds, “Prediction to Temperature Distribution and thermal History during Friction Stir Welding:Input Torque based Model”, Science and Technology of Welding and Joining, Vol. 8, pp. 165-174, 2003.

[17] P. A. Colgrove and H. R. Shercliff, “Three-Dimensional CFD Modeling of Flow around a Threaded Friction Stir Welding Tool Profile”, Journal of Materials Processing Technology, Vol. 169, pp. 320-327, 2005 eted from the biography.